GEOSCIENCE FRONTIERS 3(2) (2012) 109–124

available at www.sciencedirect.com

China University of Geosciences (Beijing)

GEOSCIENCE FRONTIERS

journal homepage: www.elsevier.com/locate/gsf

GSF FOCUS

Late Mesozoic basin and range tectonics and related magmatism in Southeast China

Dezi Wang*, **Liangshu Shu**

State Key Laboratory for Mineral Deposits Research, Nanjing University, Nanjing 210093, China

Received 31 July 2011; accepted 30 October 2011
Available online 15 December 2011

KEYWORDS
Basin and range tectonics;
Sedimentation;
Bimodal igneous rocks;
Late Mesozoic;
Geodynamic evolution;
Southeast China

Abstract During the Late Mesozoic Middle Jurassic–Late Cretaceous, basin and range tectonics and associated magmatism representative of an extensional tectonic setting was widespread in southeastern China as a result of Pacific Plate subduction. Basin tectonics consists of post-orogenic (Type I) and intra-continental extensional basins (Type II). Type I basins developed in the piedmont and intraland during the Late Triassic to Early Jurassic, in which coarse-grained terrestrial clastic sediments were deposited. Type II basins formed during intra-continental crustal thinning and were characterized by the development of grabens and half-grabens. Graben basins were mainly generated during the Middle Jurassic and were associated with bimodal volcanism. Sediments in half-grabens are intercalated with rhyolitic tuffs and lavas and are Early Cretaceous in age with a dominance of Late Cretaceous–Paleogene red beds. Ranges are composed of granitoids and bimodal volcanic rocks, A-type granites and dome-type metamorphic core complexes. The authors analyzed lithological, geochemical and geochronological features of the Late Mesozoic igneous rock assemblages and proposed some geodynamical constraints on forming the basin and range tectonics of South China. A comparison of the similarities and differences of basin and range tectonics between the eastern and western shores of the Pacific is made, and the geodynamical evolution model of the Southeast China Block during Late Mesozoic is discussed. Studied results suggest that the basin and range terrane within South China developed on a pre-Mesozoic folded belt was derived from a polyphase tectonic evolution mainly constrained by subduction of the western Pacific Plate since the Late Mesozoic, leading to formation of various magmatism in a back-arc extensional setting. Its geodynamic mechanism can compare with that of basin and range tectonics in the

* Corresponding author.
E-mail address: gxdzh@nju.edu.cn (D. Wang).

1674-9871 © 2011, China University of Geosciences (Beijing) and Peking University. Production and hosting by Elsevier B.V. All rights reserved.

Peer-review under responsibility of China University of Geosciences (Beijing).
doi:10.1016/j.gsf.2011.11.007

ELSEVIER Production and hosting by Elsevier

eastern shore of the Pacific. Differences of basin and range tectonics between both shores of the Pacific, such as mantle plume formation, scales of extensional and igneous rock assemblages and the age of basin and range tectonics, were caused mainly by the Yellowstone mantle plume in the eastern shore of the Pacific.
© 2011, China University of Geosciences (Beijing) and Peking University. Production and hosting by Elsevier B.V. All rights reserved.

1. Introduction

A *basin and range province* is a North American geomorphic-tectonic term used to describe a series of separate and parallel mountain ranges with broad valleys interposed (Dickinson, 2002). The basin and range tectonics of western North America is characterized by low-angle normal faulting (Wernicke, 1981, 1985), and metamorphic core complexes (Davis and Coney, 1979; Davis et al., 1980; Lister and Baldwin, 1993; Darby et al., 2001), developed within a previous active continental margin (Crittenden, 1980; Coney, 1980).

The North American basin and range provinces are associated with extensive magmatism, high heat flow, low seismic wave speeds and thinned crust (20–25 km thick) that is still under tensile stresses; thinned regions are surrounded by regions of compressive stresses, and there is active rifting (Miller et al., 2001). The tectonics are controlled by crustal extension in the eastern side of the Nevada magmatic arc and driven by varied geodynamic impulses (Dickinson, 2002).

As the crust stretches, faults develop to accommodate the extension. The normal arrangement in the basin and range system is that each basin is bounded on at least one side by one or more normal faults that are oriented sub-parallel to the range front (Miller et al., 2001; Darby et al., 2001; Dickinson, 2002). The formation of the basin and range tectonics of the Cordilleran belt of western North America was closely related to movement along the San Andreas transform fault at 20–30 Ma and upwelling of the Yellowstone mantle plume (Hill et al., 1992).

A similar basin-range type province occurs in the Southeast China block (SECB) that forms the Pacific coastal region of China (Huang, 1945; Xu et al., 1960; Guo et al., 1965, 1980,1989 Wang and Mo, 1995). Ren et al. (Ren, 1964; Ren and Chen, 1989) have described the varied crustal features of basin and range in China, namely, deformable crust in range and rigid crust in basin areas. Gilder et al. (1991) proposed the term "Basin and Range Tectonics of South China", in relation to the geodynamics of Late Mesozoic tectonism and granitic magmatism with basin formation due to extensional rifting in a back-arc setting associated with a subduction of the paleo-Pacific (also see Li, 2000; Zhou and Li, 2000; Zhou et al., 2006b; Shu et al., 2009a). Petrotectonics and tectonic facies of Late Mesozoic basin and range tectonics and magmatism have been elucidated by Wang and Zhou (2002) and Shu et al. (2009a,b).

Intra-continental extension leading to thinning of lithosphere and subsequent upwelling of asthenosphere (Faure et al., 1996; Shu et al., 1998; Wang and Zhou, 2002), and a combined model of subduction of the Pacific plus underplating of basaltic magma were envisaged for the formation of intra-continental igneous rock assemblages in basin and range areas (Zhou and Li, 2000, 2006).

The Late Mesozoic igneous rocks and coeval basins occupy 67% surface area of the SECB (Wang and Zhou, 2002; Zhou, 2007; Shu et al., 2009a) forming the basin and range tectonics of South China. Related granitoids host major ore deposits of W, Sn, Nb, Ta, Cu and Au (Zhou, 2007).

In this paper, geological features of the Late Mesozoic basin and range province, lithological and geochemical features of associated igneous rocks of South China are reviewed and a geodynamic model was discussed.

2. Geological background

2.1. Tectonic framework

In east Asia, the NE-trending SECB is an important tectonic unit connecting the Neo-proterozoic Jiangnan belt to the north by the Jiangshao fault zone with the East-China Sea-Taiwan–Strait to the southeast (Fig. 1). Two metamorphic units, one amphibolite facies and the other of lower-greenschist facies, and a sedimentary cover are widely developed over an area of 500,000 km^2. Based on zircon U-Pb dating, Proterozoic sandstone, claystone and volcanic rocks were metamorphosed to amphibolite facies grade at ~1.9–0.8 Ga (Yu et al., 2009; Li et al., 2010; Xiang and Shu, 2010; Yao et al., 2011), and the late Neo-proterozoic to Ordovician sandstone–claystone slaty sequence was metamorphosed to lower-greenschist facies grade at ~0.8–0.45 Ga (Li et al., 2010; Charvet et al., 2010; Shu et al., 2011).

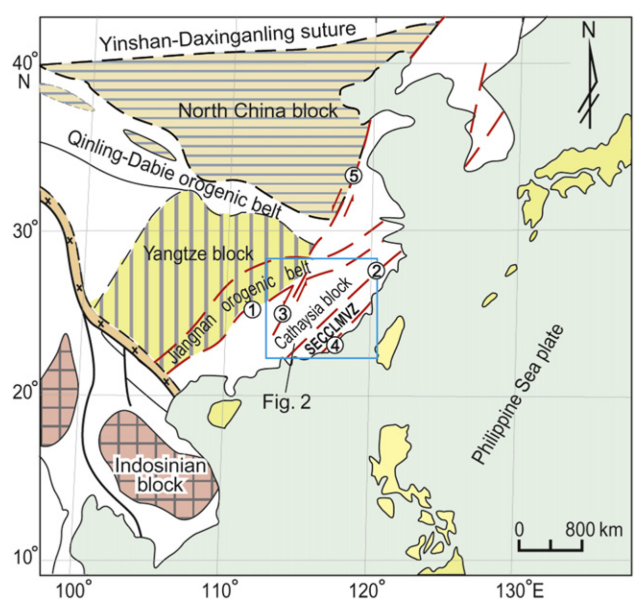

Figure 1 Tectonic framework of Southeast China. SECCLMVZ, Southeast China Coastal Late Mesozoic Volcanic Zone. ①: Shaoxing–Jiangshan–Pingxiang fault zone; ②: Zhenghe–Dapu fault zone; ③: Ganjiang fault zone; ④: Changle–Nanao fault zone; ⑤: Tan-Lu fault zone.

The Late Neo-proterozoic to Ordovician sedimentary series was intruded by Silurian granitic rocks (Zhang and Shu, 2011). Subsequently, Middle Devonian terrigenous sediments (mainly non-metamorphosed conglomerate and coarse-grained sandstone) were deposited unconformably on the Early Paleozoic rocks. This event marked the end of Early Paleozoic tectonism. Pre-Devonian metamorphic rocks are mainly distributed in the Cathaysia block (Fig. 1). In Middle Devonian to Early–Middle Triassic time, a stable sedimentary cover was formed consisting of carbonates intercalated with clastic rocks. The Late Mesozoic basin-range framework of the SECB, composed of large-scale acid volcanic-intrusive complexes and coeval sedimentary basins, was developed within the pre-Mesozoic rock areas and is distributed mainly in the Southeast China coastal zone and partly in inland areas (Fig. 2).

2.2. Lithospheric structure

Seismic data suggest that a modern flat-subduction slab occurs beneath eastern China, with magmatism in the western Pacific arc and back-arc areas caused by dehydration of the subducting slab and by liquid flow in the mantle wedge (Zhao and Liu, 2010). As a back-arc area, the SECB has a present-day crustal thickness of 29–35 km, similar to the average crustal thickness (30–35 km) of eastern China (Li, 2010). A 29–30 km-thick crust occurs beneath SE coastal areas compared with a 33–35 km-thick crust to the northwest (Xu and Shu, 2001). Tomographic imaging reveals that a distinct non-uniformity of thicknesses of the continental crust or the upper mantle occurs between the inland and coastal areas. The velocity image at 110 km depth demonstrates a marked difference from a low-speed coastal area northwestward to a high-speed region in the inland part of South China (Liu et al., 1996). This suggests that the upper limit of the asthenosphere in the coastal zone occurs at ∼110 km depth whereas the inland at the same depth still is situated within lithosphere. The upper limit of the low-resistance layer is at ∼70–80 km below the SE-China coastal region, and is 100–200 km in the inland area (Xu and Shu, 2001).

2.3. Basement structure and pre-Devonian orogenic events

2.3.1. Basement structure

The pre-Devonian metamorphic basement of the SECB is termed the ‘Cathaysia block’, and is composed of the pre-Nanhua schist, gneiss, orthogneiss and migmatite, and the Nanhua-Ordovician muddy-sandy slate series. Mafic-ultramafic rocks mark the junction between the pre-Nanhua and Nanhua-Ordovician associations and the mafic rocks are zircon U-Pb dated at 850–800 Ma (Shu et al., 2011). The Nanhua System consists mainly of intra-continental rift-type sediments and the Sinian–Ordovician sequence is characterized by a neritic-bathyal sediments, without Bouma sequence and lava. The Silurian sequence has been eroded from the Cathaysia block due to uplift since the Late Ordovician. Uplift was associated with the Early Paleozoic tectono-magmatic event that welded the Cathaysia and Yangtze blocks. This collision event was marked by regional-scale folding and faulting and granitic magmatism (Shu et al., 2008c, 2011; Faure et al., 2009; Charvet et al., 2010).

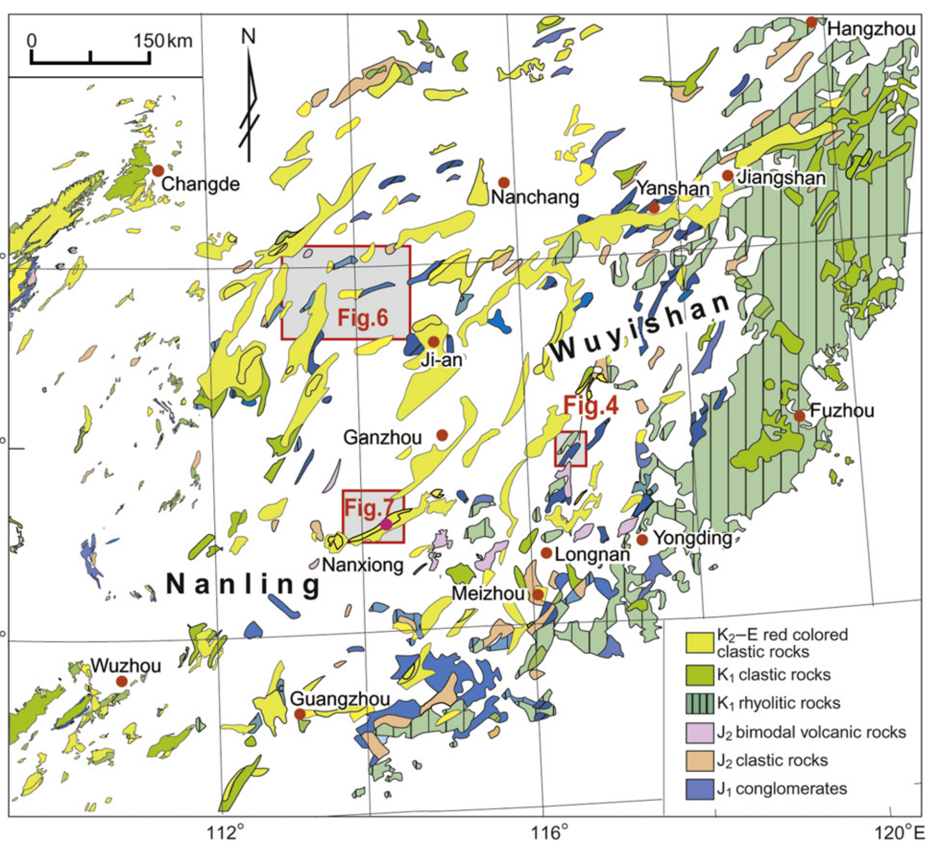

Figure 2 Map showing distribution of Jurassic–Paleogene sediments in SE China.

2.3.2. Pre-Devonian orogenic events

Based on regional-scale angular unconformities, three episodes of pre-Devonian orogeny, viz. Paleo-proterozoic, Neo-proterozoic and Early Paleozoic, have been identified in the SECB (Li et al., 2000; Yu et al., 2009; Faure et al., 2009; Rong et al., 2010; Xiang and Shu, 2010; Chen et al., 2010; Shu, 2006; Shu et al., 2008a,c 2011), corresponding to assembly of the global Columbia, Rodinia and Condwana supercontinents, respectively. The Paleo-proterozoic orogeny was mainly developed in the NE part of Cathaysia, which produced granite magmatism and amphibolites facies metamorphism, zircon U-Pb dated at ~1.9–1.8 Ga (Li et al., 2000; Yu et al., 2009). The Neo-proterozoic orogeny took place chiefly in the southern margin of the Cathaysia block, and was marked by eruption of rhyolite dated at ~0.97 Ga (zircon U-Pb; Li et al., 2005, 2010; Shu et al., 2008b 2011). The Early Paleozoic orogeny strongly influenced the entire South China, where 450–400 Ma syntectonic S-type granitoids are widely distributed (Faure et al., 2009; Charvet et al., 2010; Zhang and Shu, 2011).

A ~850–800 Ma Neo-proterozoic breakup, deduced from U-Pb zircon dating of mafic-ultramafic rocks, disrupted the Cathaysia block into several sub-terranes (Shu, 2006). Sinian–Ordovician neritic-bathyal sediments were deposited in inter-terrane basins.

2.4. Late Paleozoic sediments

During the Late Devonian–Middle Triassic, a stable shallow-sea facies of carbonates intercalated with muddy-sandy horizons, and, in some places, thin basalt layers were formed. These rocks are considered to be a part of the Tethysian regime. In the Early–Middle Triassic, a collision/orogeny along the Qinling-Dabie zone between the Yangtze and North China continental blocks strongly affected the study area. Three belts of S-type granitoids, each 30–40 km wide and covering an area of 14,300 km^2 outcrop discontinuously in the Nanling belt along E–W-trending fault zones (Zhou et al., 2006b; Sun, 2006).

Ages of the granitoids suggest that the interval from 205 to 180 Ma was devoid of magmatism (Zhou, 2007) and was followed by a transition from the Tethysian to paleo-Pacific tectonic regime (Shu and Zhou, 2002). This is indicated by a change in the direction of compressive stress from ~N–S into SE–NW associated with a change from E–W-trending Nanling bimodal-type volcanism to the formation of coastal active continental margin volcanic-intrusive complexes with a NE trend. The Early–Middle Jurassic period (~185–160 Ma) is considered to be the timing of this tectonic transition (Shu et al., 2004b).

The Late Triassic–Early Jurassic sequence with a thickness of ~600–1200 m consists of conglomerate, coarse sandstone (arkose, arkosic arenite), siltstone and claystone intercalated with coalseams. Late Triassic red conglomerate unconformably overlies Paleozoic strata, and inferred to represent a major Indosinian event.

Two types of depositional environment persisted during the Middle Jurassic, viz. fault depressions and volcanic rifts. The sedimentary sequence in fault depression consists of conglomerate, quartz sandstone, greywacke, siltstone and claystone mainly distributed in the Wuyishan area. The sequence in volcanic rifts is composed of rhyolite and basalt, forming a 600–850 m thick series distributed in the Yongding (SW-Fujian)–Longnan (S-Jiangxi)–Shixing (N-Guangdong) zone (Fig. 2).

Upper Jurassic rocks are only sparsely developed in the Meizhou–Yongding basin and are characterized by claystone and sandstone. A 650–3000 m thick Lower Cretaceous sequence consists of red ignimbrite, rhyolite lava and tuff intercalated with basalt, and in the SW-Fujian and E-Guangdong areas, Early Cretaceous black shale and sandstone with a thickness of 500–1000 m is present. Upper Cretaceous–Paleogene basins are characterized by intra-continental red-bed faulted-depressions. The Upper Cretaceous sequence is 1300–2000 m thick and consists of red conglomerate, sandstone, siltstone and claystones intercalated with gypsum and alkaline basalt dated at 97 ± 2 Ma (Shu et al., 2004a; Yu et al., 2005).

An angular unconformity occurs between the Upper and Lower Cretaceous rocks in the coastal areas of Zhejiang and Fujian Provinces (Shu et al., 2000, 2009a,b), demonstrating that the collision between Philippine Plate and East Asian continental margin affected the inland of South China (Charvet et al., 1994).

A ~800–2000 m thick Paleogene sedimentary sequence is composed of grey-red conglomerate, coarse sandstone, siltstone, claystone, and gypsum- and oil-bearing shale. Neogene rocks are poorly exposed and are characterized by brown-orange colored siltstone and claystone.

2.5. Regional fault zones

Four regional fault zones (Fig. 1) that are marked by gravity and aeromagnetic anomalies (Xu and Shu, 2001) occur in the SECB: (i) The Shaoxing–Jiangshan–Pingxiang fault zone is a ~E–W-trending Late Mesozoic feature with 40–50 km wide and ~1000 km long within which abundant blocks of Neo-proterozoic mafic-ultramafic rocks and Paleozoic carbonate rocks occur; (ii) The Zhenghe–Dapu fault zone manifests itself both as a Neo-proterozoic rift zone within the Cathaysia block (Shu et al., 2011), and also as a Mesozoic, steeply SE dipping normal fault that separates the South China Early Paleozoic fold belt to the NW from the coastal Mesozoic volcanic zone to the SE; (iii) The Changle–Nanao fault zone is a large-scale sinistral ductile shear zone within the SECB (Shu et al., 2000) that contains abundant outcrops of ~100–120 Ma orthogneiss and gneissic granodiorite (Wang and Lu, 2000). Granite magmatism occurred in response to oblique subduction of the paleo-Pacific Plate (Charvet et al., 1994), and alkaline basalts were erupted during the Late Cretaceous–Paleogene; (iv) The N–S trending Ganjiang fault zone marks the western limit of Early Cretaceous volcanic rocks. This was an intra-continental sinistral strike-slip zone during the Early Cretaceous and became a normal fault zone dipping to the east during the Late Cretaceous (Deng et al., 2003). The Ganjiang fault constrained the development and evolution of Late Cretaceous–Paleozoic fault-depression basins (Shu et al., 2009a).

3. Basic features of basin and range tectonics

3.1. Basin tectonics in the SECB

Late Mesozoic basins occupy a surface area of ~140,000 km^2 in SE China. According to a generalized classification of basin formation (Cloetingh and Podlachikov, 2000; Cloetingh et al., 2002), most basins in the SECB were formed in an extensional tectonic setting. Three types of basins can be distinguished, namely, rift basins, volcanic fault depressions and sedimentary depressions (Shu et al., 2004b, 2009a). Statistical data suggest that rift basins were mainly formed in the Early–Middle Jurassic (J_{1-2}) and are outcrop over an area of ~4600 km^2; volcanic fault-depression basins were mainly formed in the Early Cretaceous (K_1) and occupy ~85,500 km^2; sedimentary depression basins were mainly formed in Late Cretaceous–Paleogene (K_2–E) and cover an area of ~37,900 km^2 (Shu et al., 2009a) (Fig. 2).

3.1.1. Rift basins

Rift basins are exposed in the eastern Nanling area (Fig. 2) as an ~E–W-trending narrow zone. Besides Early–Middle Jurassic sand-mud rocks, the basins were filled by coeval rhyolite and basalt. Mafic dykes in granites have similar geochemistry to the basalt (Deng et al., 2003), implying the same magmatic source.

3.1.2. Volcanic fault-depression basins

These are entirely filled by Early Cretaceous volcanic rocks (e.g., tuff, dacite, rhyolite and volcanoclastics) intercalated with olivine-basalt, diabases, and granitoids of 140–110 Ma (Wang and Zhou, 2002). The basins are mainly distributed in the coastal zone of SE China and have a NE-trend and a width of 300–500 km. The thickness of the volcanic sequence is >3000 m. Locally, bimodal volcanic rocks occur in the basins, consisting of thick rhyolites and thin basalts with depleted Nb-Ta indicative of an arc petro-tectonic environment (Wang and Zhou, 2002). For example, the NEE trending Hangzhou–Jiangshan–Ganzhou fault depression (Fig. 2) is a composite basin zone with a width of 30–50 km and a length of 1000 km. It consists of many Early Cretaceous volcanic basins and Late Cretaceous–Paleogene half-grabens occupied by red beds (Yu and Xu, 1999). An ~E–W-trending translithospheric fault zone, causing basitic eruption, borders the northern margin of the basin zone, and at the southern boundary the Cretaceous strata unconformably overlie the Jurassic or Triassic sedimentary sequence (Shu et al., 2009b).

3.1.3. Red sediment-filled fault-depression basins

These basins are mainly distributed in the northern and western parts of the Wuyishan area (Fig. 2) and are characterized by a growth fault along one boundary and an angular unconformity developed at the other, forming "dustpan-like" fault-depression basins. A number of basins are bordered by translithospheric faults, which provided conduits for basalt ascent resulting in the formation of 2–20 m-thick basaltic intercalations with the basinal sediments. The basalts are dated at ~97–90 Ma (Wang and Zhou, 2002; Shu et al., 2004a; Yu et al., 2005) and show a marked Nb-Ta depletion, suggesting the presence of thick crust with a highly mature continental composition underlying the basinal areas (Shu et al., 2009a). This type of basin has various shapes and sizes, and is filled by conglomerate, coarse sandstone, siltstone and claystone.

3.2. Range tectonics

Granitoids and several metamorphic core complexes or granitic domes were formed in Middle–Late Jurassic and Early Cretaceous and built the towering range landform of SE China. Four ranges are distributed in the SECB. They are, from the coast to the inland: (1) The NE-trending Daiyunshan–Bopingling range of Central Fujian with the highest point of 1856 m, consisting mainly of Early Cretaceous granite bordered by coeval volcanic fault depressions; (2) The NE-trending Wuyishan range of northern Fujian–central Jiangxi with 13 peaks of more than 1500 m, the highest of which is Huanggangshan at 2158 m, and composed of Early Cretaceous granite in contact with pre-Devonian metamorphic basement. The Hangzhou–Dongxiang Cretaceous–Paleogene basin zone occurs in its northern side, and a coastal Early Cretaceous volcanic basin zone is situated in the SE of the range; (3) The ~E–W-trending Wugongshan range covering an area of ~3000 km^2 and including Jinding Peak (1918 m). This is a Mesozoic metamorphic core complex composed of six Early Cretaceous granitic bodies and Proterozoic metamorphic rocks in the core, with the Pingxiang and Anfu basins on the northern and southern sides, respectively. Two main detachment faults occur between the core complex and the basins; (4) The sub-E–W-trending Nanling range (Fig. 2) bordered by Triassic–Jurassic sedimentary basins. The range is composed of three E–W-trending Indosinian and early Yanshanian granitic zones with a width of ~300 km, forming 10 peaks of 1000–1500 m including famous "Five Ranges", namely, the Dayu Range, the Qitian Range, the Yuecheng Range, the Mengchu Range and the Doupang Range. Shikengkong, the highest peak of 1902 m, is situated on the boundary between the Hunan and Guangdong provinces.

3.3. Coupling relationship between basins and ranges

Large-scale granitic magmatism and basin tectonics have resulted from crustal extension. Many extensional faults were developed in the coupling zones of basins and ranges. The granitic ranges occur together with basins and have similar or a slightly older age than the basins. Thus, the ranges were the provenances of the coarse, granitic detritus of the basin sediments. Sedimentary basins are bordered by extensional faults. There are four types of basin-range coupling relationship in the SECB: (1) *graben-type*: both boundaries of a basin are in contact with granitic ranges by normal faults dipping toward the center of the basin, as seen in the Linjiang–Dongkeng basin of southern Jiangxi of the eastern Nanling area (Fig. 2); (2) *half-graben type*: here a normal fault acts as the single boundary between the basin and the granitic range, whereas the other boundary of the basin is an angular unconformity. Mafic dyke swarms and olivine-basalt lavas are frequently developed along a large normal fault, as seen in the Nanxiong basin of the east Nanling area; (3) *Symmetric metamorphic core complex* (*MCC*) *type*: this type shows a back to back slipping pattern and often occurs in the metamorphic core complex. Taking the Wugongshan core complex as an example, two slopes of complex are in normal fault contact with the Pingxiang and the Anfu basins; (4) *The strike-slip type*: the Changle Early Cretaceous volcanic basin is connected to the coeval granitic range by a sinistral strike-slip fault (Shu et al., 2000).

4. Features of extensional igneous associations

Igneous rocks associations of the extensional setting in the SECB are characterized by different areal extents, distinct provenances and complex origins. They are mainly granitoids with outcrop areas similar to those of the basins. The granitoids invariably coexist with bimodal rhyolite-basalt volcanics, composite intrusives, mafic and felsic dyke swarms, shoshonites, metamorphic core complexes and minor alkaline rocks (Wang and Zhou, 2002; Zhou, 2007).

4.1. Granitoids

Late Mesozoic granitoids occupy an area of ~140,000 km^2 (Fig. 3) and were mainly formed in the Middle–Late Jurassic (176–146 Ma, J_2–J_3) and Cretaceous (146–66 Ma, K). A significant time–space evolution trend of granitic magmatism was detected (Zhou et al., 2006b; Zhou, 2007), i.e., from the SECB

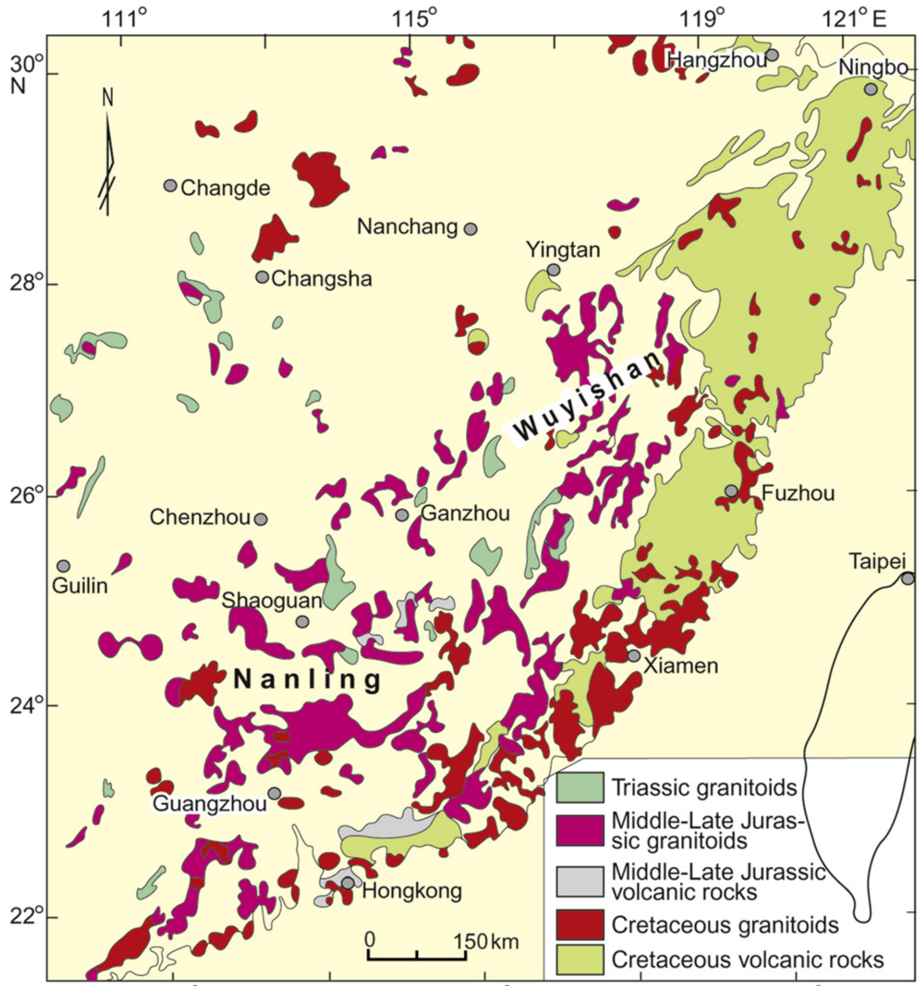

Figure 3 Map showing distribution of Mesozoic granitic rocks in the SECB (modified from Zhou et al., 2006b).

inland eastwards, granites gradually become younger in age and larger in size.

Peraluminous granitoids (biotite granite, K-feldspar granite and two-mica granite) are mostly developed in the Nanling Range (Figs. 2 and 3), of Middle–Late Jurassic age and are locally of Cretaceous age. The granite outcrops are arranged parallel the ∼E–W-trending ranges. In the Dingnan–Longnan areas of southern Jiangxi of the eastern Nanling area, Early–Middle Jurassic granites are exposed and coeval rhyolitic rocks occur in the neighboring basins. Toward the E, the ∼E–W-trending peraluminous granites become younger (Fig. 3) (Shu et al., 2004b).

Geochemical studies suggest that the granitic volcanic-intrusive complexes of the SECB can be divided into two types, I- and S-type. Large-scale I-type volcanic-intrusive complexes were mostly formed during the Early Cretaceous and are widely distributed in the coastal region of SE China. The smaller scale S-type volcanic-intrusives are mainly 140–110 Ma (K_1) (Wang and Zhou, 2002). The other S-type plutons with U-Pb age of 160–150 Ma (Late Jurassic; J_3) are exposed only in the northwestern Wuyishan zone (Fig. 3) such as in the Yanbei and Lengshuikeng areas. In the Xiangshan area of inland, Early Cretaceous S-type rhyolites contain magmatic original andalusite and garnet. These rhyolites coexist with coeval S-type granite to form the Xiangshan granitic volcanic-intrusive complex (Wang and Shen, 2003).

In the SE China coastal region, most granitoids are I-type granodiorite and granite. Porphyritic and massive varieties are mostly Early Cretaceous with a few formed during the Late Cretaceous. Large-scale NE-trending granitoids coexist with coeval volcanic basins where the transition from granite to rhyolite constitutes a continuous sequence both vertically and horizontally. Vertically, welded tuffs and rhyolites occur in the upper part and granites in the lower part. Geochronology and stable isotope data clearly indicate the coeval and co-source relationship between the I-type granite and rhyolite complexes (Wang and Zhou, 2002). Zhou and Li (2000) proposed a subduction-underplating model to interpret the petrogenesis of the I-type granites. This involves thermal softening and partial melting of the middle–lower crust in the hanging wall of the subduction slab, melting of the subduction slab in the deeper crust, and/or underplating of basaltic magma along an extensional fault.

4.2. Bimodal volcanic rocks

Bimodal volcanic rocks developed during Early–Middle Jurassic (J_{1-2}) and Cretaceous (K) (Wang and Zhou, 2002; Chen et al., 1999, 2002; Deng et al., 2003; Shu et al., 2009a), and occur in at least sixteen Mesozoic basins. The J_{1-2} bimodal volcanic rocks are distributed in the inland; the Cretaceous ones are concentrated in the coastal areas and show evidence of mixing between crustal and mantle material, suggesting an upper mantle–lower crust derivation of the magmas.

4.2.1. Early–Middle Jurassic bimodal volcanic rocks

These form an E–W-trending volcanic series with a thickness of ~800–1200 m consisting of approximately equal volumes of basalt and rhyolite. The volcanic association is extensively developed along the SW-Fujian–S-Jiangxi–S-Hunan zone of eastern Nanling (Fig. 3) with a length of ~250 km and a width of ~30–40 km. The interbedded basalt and rhyolite occur in the upper part of the volcanic sequence and interbedded basalt and arkose occur are in the lower part. The volcanic series has geochemical features indicating intra-continental magmatism (Zhou and Chen, 2000, 2001).

The basalts and rhyolites are U-Pb dated at 185–170 Ma and 180–160 Ma, respectively. For example, basalt and rhyolite of the lower parts of the Yongding, Xunwu and Longnan basins yield ages of 185 ± 5 Ma, 178 ± 7 Ma and 173 ± 6 Ma, respectively (Chen et al., 1999; Zhou et al., 2005, 2006a,b), and rhyolite of the upper part of the Longnan basin (Fig. 4) yields a SHRIMP zircon U-Pb age of 160 ± 1 Ma (Shu et al., 2009b). Early–Middle Jurassic bimodal granite and gabbro of 196–165 Ma (Yu and Shu, 2004; Yu et al., 2009), also crop out in the Nanling area, and show similar geochemical features to coeval volcanic rocks.

A NW–SE section measured in the Dongkeng–Linjiang rift basin in South Jiangxi (Fig. 4) shows that the basin is filled by the Lower Jurassic Linshan and Middle Jurassic Changpu Formations. The Linshan Formation is 1200 m thick consisting of conglomerate, coarse sandstone, arkose and quartz sandstone in the lower part, and sandstone and siltstone intercalated with coal beds in the upper part. The Changpu Formation is ~1300 m thick and mainly composed of basalt, basic tuff, rhyolite and rhyolitic tuff intercalated with sandstone containing animal- and plant fossils of Middle Jurassic age (Deng et al., 2003). The basaltic- and the rhyolitic rocks are approximately the same thickness. Basalt from the lower part of the Yuezi–Liren section in the Longnan County (Fig. 4) is Rb-Sr dated at 178 ± 7 Ma (Chen et al., 1999) and a SHRIMP zircon U-Pb age of 160 ± 1 Ma is obtained from rhyolite from the upper part of the section (Shu et al., 2009b), constraining the forming time of this basin.

Black and green basalts show aphanitic texture, and contain 10% phenocrysts of labradorite, pyroxene and olivine. These also display amygdaloidal and massive structures. Glassy matrix has been weakly metamorphosed to a mixture of fine-grained chlorite, feldspar and calcite. Vesicles form ~10%–25% volume of the basaltic rocks and are filled by chlorite, prehnite and opal. The vesicles are all elongated along a NE-direction, implying a syntectonic deformation during extensional rifting (Shu et al., 2009a).

Red-colored rhyolitic rocks have porphyritic texture and rhyotaxitic structure. Phenocrysts (often embayed by resorption) consist of sanidine, orthoclase (10%), quartz (10%) and albite (2%). The matrix consists of microcrystal feldspar and quartz aggregates (Deng et al., 2004; Shu et al., 2009a). Geochemically, basalts from the Yuezi–Liren section have $w(TiO_2)$(2.23%–2.87%), $w(SiO_2)$(49.43%–50.68%), $w(Na_2O)$(2.5%–3.8%), Na_2O/K_2O >1.6; low LREE's, slightly depleted Eu, and low Nb, Zr, Th, Y, and can be classified as intra-continental tholeiite. Rhyolitic rocks have high $w(SiO_2)$(67.81%–76.8%), $w(Al_2O_3)$(11.72%–14.52%)

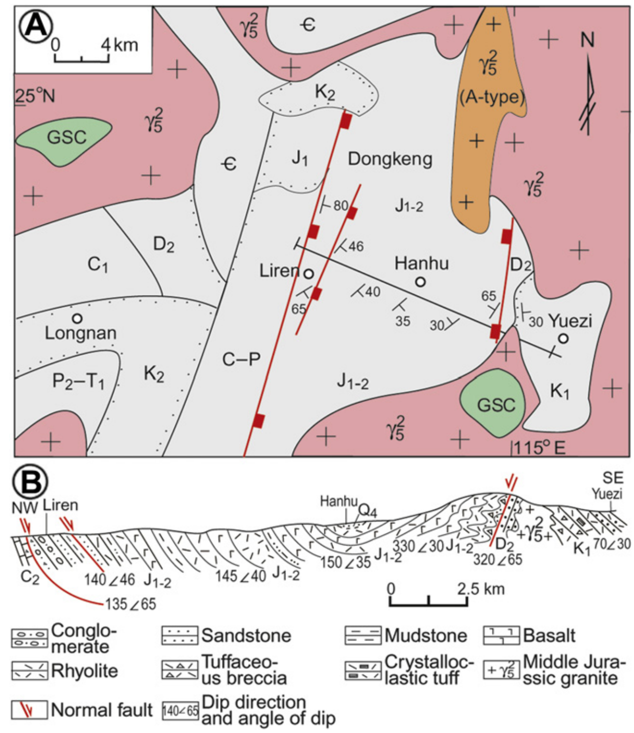

Figure 4 Geological map of the Dongkeng rift basin (J_{1-2}). Abbreviations: Є, Cambrian sandy-muddy slates; D_2, Middle Devonian conglomerate and coarse sandstone; C_1, Early Carboniferous clastic rocks; C–P, Carboniferous–Permian limestone intercalated with clastic rocks; P_2–T_1, Late Permian–Early Triassic limestone and claystone; J_1, Early Jurassic conglomerate and coarse sandstone; J_{1-2}, Early–Middle Jurassic rhyolite and basalt intercalated with sandstone and claystone; K_1, Early Cretaceous rhyolitic tuffs; K_2, Late Cretaceous sandstone, siltstone and claystone; GSC, Middle Jurassic gabbro-syenite complex.

and $w(K_2O)$(4.34%–6.31%) with ANKC >1.1, K_2O/Na_2O >1.5, high $\sum$REE and LREE's, high Rb and Th, low Ba and Ti, marked negative Eu anomalies, and may be classified as high-K peraluminous rhyolites generated in an intra-continental rifting setting (Deng et al., 2004; Shu et al., 2009a).

4.2.2. Cretaceous bimodal igneous rocks

Most rocks of this magmatic association were formed in the late Early Cretaceous. Locally, bimodal volcanic rocks coexist with bimodal intrusives and A-type granites, and represent typical extensional magmatic rocks. The bimodal association is mainly developed in the coastal areas of the Zhejiang and the Fujian provinces, especially in the NE-trending Changle–Nanao fault zone (Fig. 5).

Different from the Jurassic bimodal volcanic series in the inland area, the rhyolite formed in the coastal areas during the late Early Cretaceous is the dominant member (more than 90%) of the bimodal igneous assemblage, these basalt and rhyolite were produced at the time 110–100 Ma, e.g., 111 Ma for basalt and 101 Ma for rhyolite in the Ningbo basin of SE Zhejiang; and 107 Ma for tholeiite basalt and 108 Ma for rhyolite in the Yongtai basin of SE Fujian (Wang and Zhou, 2002). Geochemically, tholeiitic basalts are notably depleted in Nb and Ta, indicative of an active continental margin petrogenetic setting. The tholeiitic

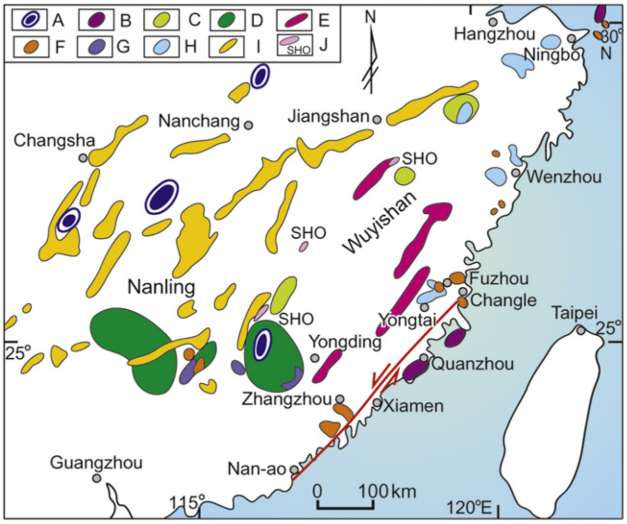

Figure 5 Petrotectonic assemblages of Southeast China Late Mesozoic extensional tectonics (modified from Zhou et al., 2006b). A—Metamorphic core complex; B—Mafic dyke swarms (K_1); C—Felsic dyke area of concentration (J_3–K_1); D—Mafic dyke area of concentration (J_3–K_1); E—Porphyroclastic lava belts (K_1); F—A-type alkaline and miarolitic granites (K_1 in coastal areas and J_2 in Nanling Range); G—bimodal volcanic rocks (basalt nearly equal to rhyolite in thickness, J_2); H—bimodal volcanic rocks (rhyolite much thicker than basalt, K_1); I—red-bed basins (K_2–E, formed mainly in K_2, basalt-bearing in some basins); J—Shoshonites (K_1).

basalts are distinct from the Jurassic rift-type basalts described above. Interestingly, rhyolites show negative $\varepsilon_{Nd}(t)$ values and Meso-proterozoic T_{DM2} ages of 1.4–1.2 Ga (Wang and Zhou, 2002), suggesting either the addition of juvenile mantle materials or the result of crust-mantle interaction.

The Cretaceous bimodal plutonic assemblage is characterized by a mafic and felsic dyke swarm and composite bodies of granite and gabbro. The dyke swarm is seen in the coastal areas of Zhejiang (Fig. 5) where it is composed of diabase (~50–300 cm thick) and granitic porphyry. The composite bodies of granite and gabbro are widely distributed in the coastal areas of Fujian, e.g., Zhangzhou, Quanzhou, Pingtan Island and Tongan areas, where the large outcrops of granite are associated with small bodies of coeval gabbro (Zhou and Chen, 2001).

4.3. A-type granite

A ~800 km long, ~60–80 km wide zone of Late Cretaceous A-type granite occurs in the coastal region of Fujian and Zhejiang (Fig. 5). The zone includes miarolitic granite, alkaline granite and shoshonite along or close to the Changle–Nanao fault zone. In some cases, A-type granites coexist with I-type granites, forming I–A composite plutons, e.g., Fuzhou, Zhangzhou, Zhoushan and Qingtian composite bodies. In the I–A composite plutons, I-type granites are U-Pb dated at 130–100 Ma and A-type granites have an age range of 90–100 Ma (Wang and Zhou, 2002).

A-type granite commonly contains geodes that are inferred to reflect a shallow emplacement. According to mineralogy and geochemistry, the A-type granites can be divided into peralkaline and aluminous types (Qiu et al., 2000a, 2004). Aluminous A-type granite is predominant, and quartz and alkaline feldspar are the main minerals of both types. In the coastal areas of the SECB, aluminous A-type granite often contains biotite and minor plagioclase, while peralkaline A-type granite is poor in plagioclase but contains aegirine and arfvedsonite (Wang et al., 1995).

Geode minerals are different for the two types of A-type granite. Garnet and muscovite are dominant minerals in geodes of aluminous A-type granites, whereas the alkaline Fe-Mg silicates aegirine and arfvedsonite often fill geodes of the peralkaline A-type granite. Evidence from accessory minerals indicates that the peralkaline A-type granites originated from a greater depth greater than the aluminous A-type granites, and the former were generated from addition of more mantle material (Qiu et al., 2004). A-type rhyolites are also found in the bimodal volcanic association near Yongtai, 60 km from Fuzhou (Fig. 5) (Qiu et al., 2000b).

A close genetic relationship occurs between the bimodal volcanic series and A-type granite. A-type rhyolite with a mineral–rock Rb-Sr isochron age of 104.1 Ma occurs at the top of the Yongtai bimodal volcanic section. Nearby, the Kuiqi A-type granite of Fuzhou is dated at 93 Ma. Both rhyolite and granite are nearly coeval and have a common mixed crust-mantle magma provenance (Wang and Zhou, 2002).

4.4. Cordilleran-type metamorphic core complexes and hot granitic domes

Our previous study (Wang et al., 2001) suggested that a cordilleran-type extension tectono-magmatic assemblage was developed in the SECB. This included metamorphic core complexes (MCC) and hot granite domes that were the result of crustal thinning, underplating of basaltic magma, partial melting of continental crust, interaction between crust and mantle, uplift and expansion of granitic magma (balloon effect) (Shu et al., 1998; Wang et al., 2001). Intersections of two regional-scale faults provided conditions for the formation of dome-like structures. Regional-scale transcrustal detachment faults between basins and ranges were loci for the formation of metamorphic core complexes and hot dome tectonics (Shu et al., 1998).

The metamorphic core complexes and hot granite domes are characterized by a core of granite and metamorphic rocks that form ranges, asymmetric extensional basins or fault depressions on both sides of the ranges, and detachment faults between basins and ranges. Basalts in basins have the same age and similar geochemistry to the continental rift-type basalt dyke swarms that intruded the granite of the ranges. A distinct difference between the metamorphic core complexes and hot granite domes is their depth of formation. The former was formed at depths >10 km due to deep thrust faults cutting middle–lower crust rocks and moving slabs of Proterozoic basement upward and forming extensional-type ductile shear zones ~30 km thick, as seen in the Wugongshan area (Fig. 6) (Wang et al., 2001). These ductile shear zones are about 2–3 km wide formed within the upper crust at 5–10 km. Consequently, rare Precambrian basement rocks reached the surface along major detachment faults. The hot granite domes are only developed near these detachment faults, as shown in the Zhuguang, Hengshan and Taoxi areas (Shu et al., 1998, 2004a).

4.4.1. The Wugongshan metamorphic core complex

This core complex is located at the intersection between the Ganjiang- and Jiangshan–Pingxiang faults, within Cathaysian Proterpozoic basement and the E–W trending Early Paleozoic fold belt. It occupies an area of ~3000 km^2.

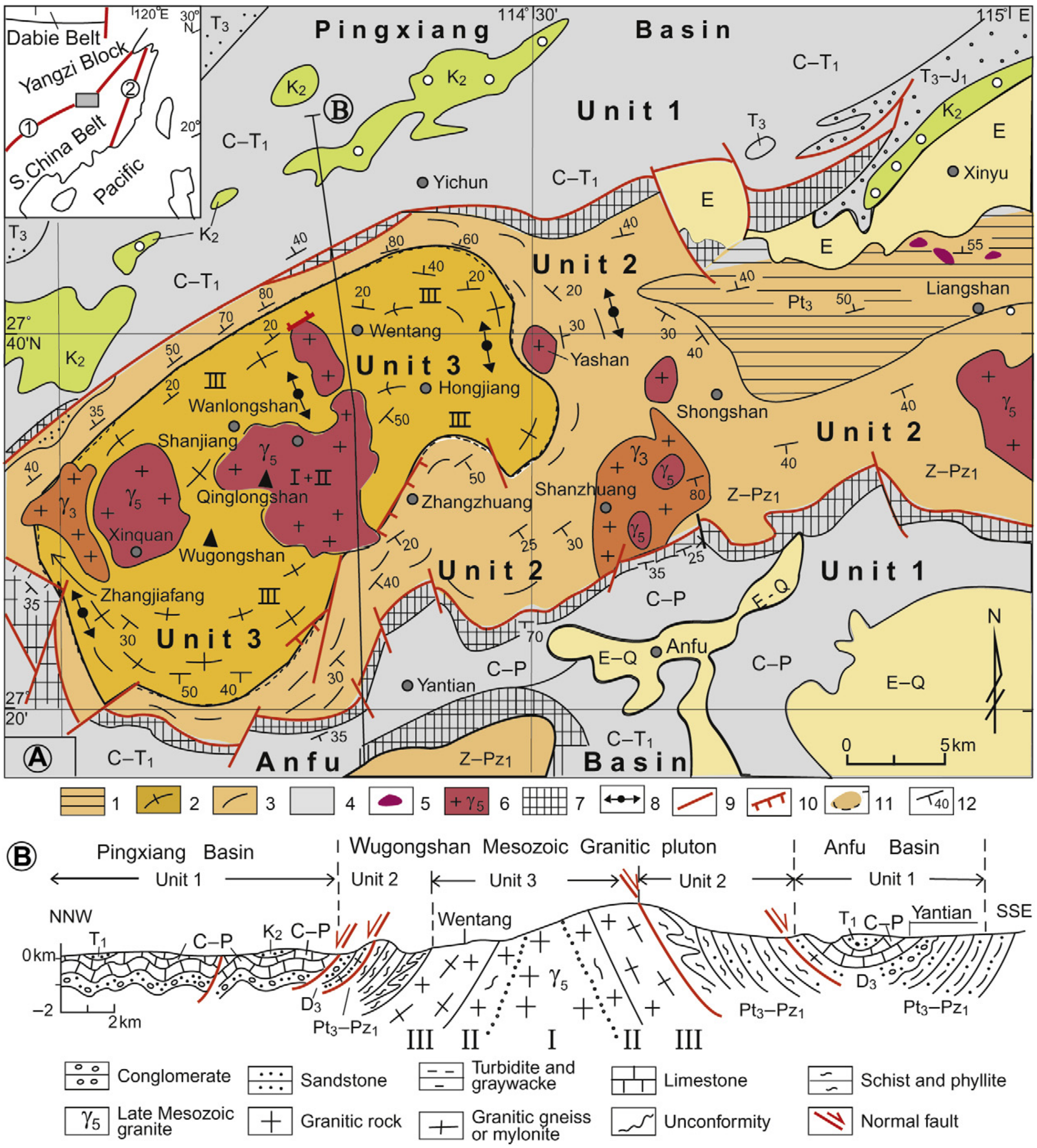

Figure 6 Simplified geological map of the Wugongshan area with a geological section throughout the Wugongshan pluton, Pingxiang and the Anfu basins. 1—Neo-proterozoic schistose volcanoclastic rocks with ultramafic blocks; 2—granitic gneissic rocks (Zone III of Unit 3); 3—micaschist and phyllite within Unit 2, and slate-phyllite-schist series surrounding the core complex; 4—folded Late Paleozoic to Early Mesozoic sedimentary strata; 5—ultramafic block; 6—Yanshanian granite (Zones I and II in the inner rim of the core complex) and oriented porphyritic K-feldspar granites (Zone II); 7—weakly mylonitized Devonian quartzite and quartz sandstone; 8—coaxial shear along lineation; 9—large detachment ductile fault; 10—ductile normal fault; 11—boundary between Unit 2 and Unit 3; 12—foliation.

A ∼N−S-direction section across the Wugongshan metamorphic core complex is shown in Fig. 6A. The complex is composed of a brittle deformed upper detachment unit that consists of N−S trending normal faults, and the folded and fractured Pingxiang and Anfu basins filled by Late Paleozoic−Mesozoic limestone and sandstone (Unit 1); a ductile deformed lower detachment unit composed of greenschist facies Early Paleozoic to Sinian slate and phyllite (Unit 2); a core of Late Mesozoic syntectonic granite surrounded by Indosinian gneissose granites (Unit 3), muscovite Ar-Ar dated at 225−235 Ma (Faure et al., 1996; Shu et al., 1998; Wang et al., 2001). Sillimanite, garnet, muscovite and biotite occur in schists and orthogneisses of this unit, indicating higher greenschist-amphibole facies metamorphism.

Unit 3 can be divided into three lithological zones (Fig. 6B), a core of granites with prophyritic to massive granite (Zone I), an intermediate zone (Zone II) of gneissic granite containing sillimanite, garnet and aligned euhedral feldspar phenocrysts, and an outer granitic gneiss, migmatite and micashist zone (Zone III) (Wang et al., 2001). A basic dyke swarm and mafic enclaves occur near the main detachment fault, suggesting the effects of basalt underplating and crust-mantle interaction (Wang et al., 2001). Two large ductile listric normal faults are developed between Units 1 and 2, i.e., a northern detachment fault and a southern detachment fault.

All the pre-Devonian strata form an anticlinorium structure with an E−W trending axial zone through the Hongjiang−Wanlongshan area (Fig. 6A). A ductile shear zone defines the foot wall (Units 2 and 3) of the main detachment fault and consists of mylonitized migmatite, gneisse and schist. A brittle shear zone forms the hanging wall (Unit 1) of the main detachment fault and is composed of imbricated normal faults. Both the hanging- and foot-walls of the main detachment fault have similar geometric and kinematic features, indicating that the fault represents a collapse structure towards the basins from the range or core part of the complex (Faure et al., 1996; Shu et al., 1998).

Granitic magmatism occurred during the Early Paleozoic and Cretaceous. The former granites are exposed in the Shanzhuang, Zhangzhuang, Hongjiang and Zhangjiafang areas (Fig. 6A), and comprise orthogneiss, gneissic granite and granodiorite zircon U-Pb dated at 460 ± 2 Ma and 428 ± 1 Ma (Lou et al., 2005). These rocks form the outer zone (Zone III) of Unit 3. The central zone (Zone 1) of Unit 3 consists of six K-feldspar granite bodies containing sillimanite, garnet, muscovite and biotite, with the Qinglongshan and Wentan granite bodies U-Pb zircon dated at 123 ± 2 Ma, 126 ± 6 Ma, 130 ± 3 Ma, 132 ± 2 Ma (Faure et al., 1996; Wang et al., 2001; Lou et al., 2005).

The lithofacies of the three zones of Unit 3 are continuous. However, each zone has different characteristic minerals. Taking the Qinglongshan body as an example, sillimanite in Zone I, garnet in Zone II, and biotite and muscovite in Zone III, suggest that Zone I represented the highest temperature part of the crystallizing granite magma. The evolution of rock structures is also very clear in the three zones, ranging from massive in Zone I through aligned porphyritic in Zone II to gneissic or schistose in Zone III, demonstrating progressively stronger ductile shearing towards the margin of the granite body. Away from the granite, metamorphism and ductile deformation weaken, suggesting that; (1) the granitic magma provided the heat as one of the triggers of ductile deformation of the Wugongshan MCC, and (2) metamorphism and ductile deformation of the core complex were constrained by the high-temperature core area of the granite magma and the main detachment fault.

Geochemical studies show that the Early Paleozoic granodiorites are of calc-alkaline affinity and characterized by lower SiO_2 with andesine, biolite, quartz, hornblende, magnetite and titanite. The Mesozoic felsic plutonic rocks are S-type, high-K granites with high SiO_2, Al_2O_3, K_2O, Rb, Zr, Th, low Eu, Ba, Nb, with LREE-enriched patterns and marked negative Eu anomalies. The Wugongshan Late Mesozoic granites have higher I_{Sr} values (0.70981−0.72885) and lower $\varepsilon_{Nd}(T)$ (−10.6 to −14.7) than the Shanzhuang Early Paleozoic granodiorite (Fig. 6), indicating higher crustal maturity. The Late Mesozoic granitoids are zoned reflecting that they resulted from the partial melting of sedimentary rocks. It is an evidence that most granite magmas are formed by the partial melting of sediments plus or minus igneous/metamorphic rocks; granites are more likely zoned due to the effect of crystallization from center to margin of a magma body.

$^{40}Ar/^{39}Ar$ and the U-Pb dating of the Wugongshan MCC indicate two Mesozoic geodynamic events causing intra-continental deformation and magmatism. The earliest tectonothermal event, dated at 225−235 Ma by $^{40}Ar/^{39}Ar$ of muscovite or biotite from granitic gneisse in the outer zone of Unit 3 (Faure et al., 1996), is linked to Indosinian collision between the South China and North China plates during the Triassic. The second event took place during the Early Cretaceous, dated at 132−123 Ma by zircon U-Pb dating of granite of the core of Unit 3 (Wang et al., 2001; Lou et al., 2005), was responsible for final doming of the Wugongshan plutons. Thus, the formation of the Wugongshan MCC may be connected with crustal extension, caused by the NW-ward subduction of the paleo-Pacific Plate beneath the SE-China continent along the SW Japan−Taiwan zone during the Late Jurassic−Early Cretaceous (Faure et al., 1996; Charvet et al., 1999; Wang et al., 2001; Shu et al., 2009a).

4.4.2. Zhuguang hot doming extensional tectonics

Located at the intersection of the Nanxiong and Wuchuan-Sihui faults (Fig. 7), the E−W-trending Zhuguang extensional hot dome is a Late Mesozoic basin and range feature developed in pre-Devonian basement and Early Paleozoic fold belt (Shu et al., 2004a). The dome is composed of the Late Cretaceous Baishun granite, the Nanxiong and Rucheng basins, and a NE-trending major detachment fault that cuts Late Paleozoic rocks and poly-stage granites (Fig. 7A, B).

The slip direction of the main detachment fault is regionally consistent. With the E−W-trending Baishun granite as a core, the two limbs exhibit a slip shearing (top-to-the-north) toward the coeval Rucheng basin for the northern limb and top-to-the-south shear direction toward the Nanxiong basin on the southern limb (Fig. 7), indicating doming extension during Late Cretaceous.

The Zhuguang Range is composed of Precambrian metamorphic rocks (schist and gneiss with sedimentary and igneous protoliths) and composite granitoids of Early Paleozoic (γ_3), Triassic (γ), Late Jurassic−Early Cretaceous (γ) and Late Cretaceous (γ) ages (Fig. 7). Late Cretaceous granites form the Zhuguang complex and comprise small-scale surface granitic bodies that represent the outcrops of an irregular upper surface of a much larger, regional-scale granite layer at depth. These bodies transect older granitoids to produce dome-like structures.

The earlier granitic plutons are zircon U-Pb dated at 140−160 Ma (Xu et al., 2003; Deng, 2003), and the later granitic bodies have U-Pb ages of 104−95 Ma (Deng, 2003) consistent with a Sm-Nd age of 94 ± 7 Ma of basic dykes that intrude the granite (Chen et al., 1998). The Nanxiong basin that borders the granite range is filled by Late Cretaceous red beds and interlayered olivine-basalt with zircon U-Pb age of 96 ± 1 Ma (Shu et al., 2004a), and therefore similar to ages of the Late Cretaceous Baishun granite and basic dykes.

Rocks surrounding the Zhuguang plutonic complex are mainly Neo-proterozoic−Paleozoic sedimentary rocks. In contrast to the Wugongshan MCC, the associated ductile shear zone is only 2−3 km wide and is developed only in or near the main detachment fault due to emplacement of the Late Cretaceous granite. Further from the main fault, evidence of ductile shearing abruptly disappears and is replaced by brittle deformation (Shu et al., 2004a).

Taking the Nanxiong fault as the main detachment fault (Fig. 7B), the hanging wall (SE-wall) is a ∼2000−3000 m thick

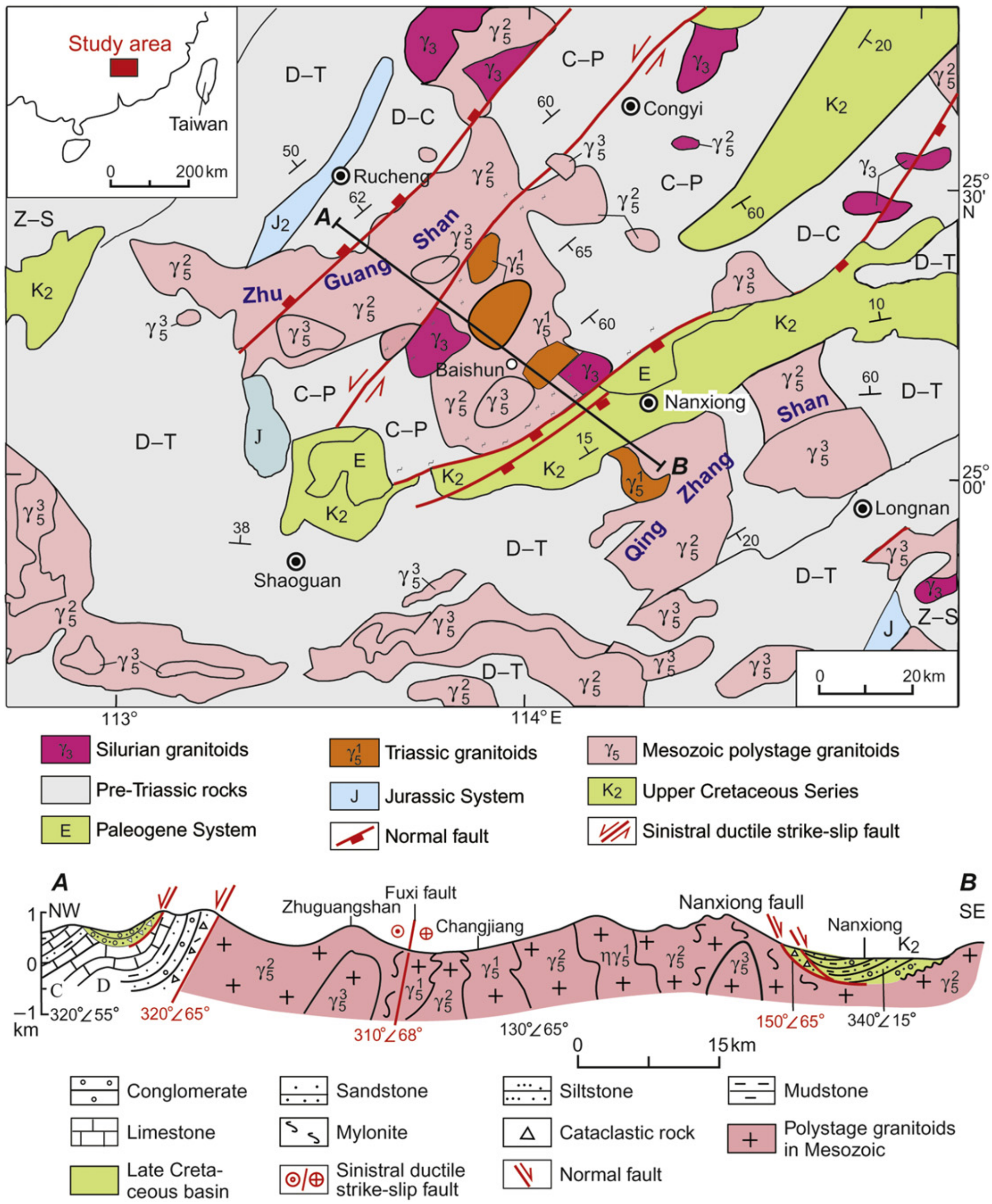

Figure 7 Geological map and NW–SE section of the Zhuguang granitic and Nanxiong Late Cretaceous half-graben basin, northern Guangdong Province.

brittle deformed zone, and the foot wall (NW-wall) is a ~1800–2500 m ductile deformed zone. From the Baishun granite toward the Nanxiong basin, the deformed zones are successively porphyritic granite zone → gneissic granite zone (1200 m wide) → orthogneiss zone (800 m) → transcurrent felsic mylonitic zone (20 m, the uppermost part of the foot wall) → silicified rocks and silicified breccia zone (50 m, the basal part of the hanging wall) → red breccia rubble zone (100 m) → red carbonation alteration zone (0.5–1.0 m wide) → red sandy gravel zone, showing a regular evolution of deformation (Shu et al., 2004a).

The Late Cretaceous granites consist of porphyritic microcline granite and muscovite-biotite granite. Geochemically, they are characterized by high SiO_2, Al_2O_3, and K_2O, alkalinity index > 2.8, ANKC > 1.1, LREE and Rb, Zr, Th enrichment, high REE, marked negative Eu anomalies, depletion in Ba and Nb, negative $\varepsilon_{Nd}(t)$ values (−10.6 to −11.5) (Shu et al., 2004b), and are inferred to have been derived from partial melting of continental crustal rocks.

Mafic dykes and enclaves are abundant. The mafic enclaves show typical characteristics of mixing of basic and acid magmas, which is considered to have been caused by basalt underplating. Basaltic rocks in the basin have similar isotopic ages and geochemical features with mafic dykes in the granitic range. Basalt flows and dykes have positive $\varepsilon_{Nd}(t)$ values (+2.6 to +4.9) (Shu et al., 2004a), reflecting a depleted upper mantle source.

4.5. Other igneous rocks

A small outcrop of aegirine-bearing granite occurs in the Ejinao segment of the Nanling belt (Zhou, 2007) that coexists with syenite and gabbro. The syenite is dated at 127.5 Ma (Bao et al., 2000). Several shoshonite bodies are sporadically exposed in the NE-Jiangxi–SW-Fujian areas (Fig. 5). Felsic and mafic dyke swarms, dated at Late Cretaceous (K_2), are widely distributed in the coastal Ningbo, Wenzhou, Fuzhou, Dehua and Quanzhou areas (Fig. 5), and indicate an intra-continental extensional petrotectonic setting (Wang et al., 1995; Wang and Zhou, 2002).

5. Formation and evolution of Late Mesozoic basin and range tectonics

Before the Jurassic, most areas of the inland part of the SECB formed part of the E–W-trending Tethys terrane within which the Late Mesozoic basin and range province developed. Since the late Early Jurassic, the Tethys tectonic regime was gradually replaced by paleo-Pacific tectonic regime, with the initiation of extensional-type basin and range tectonics of the SECB. The formation and evolution of the Late Mesozoic basin and range terrane are summarized in Fig. 8.

5.1. Early–Middle Jurassic ($J_{1\text{-}2}$): transition stage of tectonic regimes

The basin and range terrane of South China was developed on the Cathaysian block that mainly consists of Precambrian basement and Paleozoic meta-sedimentary rocks. Since the Mesozoic, two depositional regimes, the Tethysian and paleo-Pacific, have co-existed in the SECB. The Tethysian regime is characterized by approximately an E–W-trending carbonate and flysch sequence; the paleo-Pacific regime is characterized by the deposition of terrestrial volcaniclastic rocks and red beds in NE-trending faulted-depressions. In the Nanling belt, three 30–40 km wide S-type granitoid zones dated at 240–205 Ma and 180–150 Ma (Zhou et al., 2006b) occur along sub-E–W-trending fault zones, and are considered to be a part of the Tethysian regime, or a result of post-collision in the Tethysian belt (Shu et al., 2009a,b).

Since the Early Jurassic, subduction of the paleo-Pacific Plate beneath the eastern Asian margin along the Japan Trench has occurred. Even if the amount of subduction did not initially extend to the SECB, coastal areas of South China were affected as indicated by uplift of the Wuyi range, as evidenced by the deposition of Middle Jurassic conglomerate on the northern side of the range (Shu et al., 2009a,b). Subsequent deformation yielded by paleo-Pacific Plate subduction caused re-mobilization of intra-continental faults formed during Tethysian time and magmatism.

In the eastern Nanling area, six bimodal E–W-trending volcanic basins with an isotopic age of 185–160 Ma ($J_{1\text{-}2}$) (cf. Fig. 2) form a key bimodal volcanic zone occupying an area of 4600 km^2 within the former Tethysian regime. Coeval alkaline syenite–gabbro–granite has been reported in the Nanling area (Zhou, 2007), where the syenite has a wide range of Sr and Nd isotopic compositions ($I_{Sr} = 0.7032–0.7082$, $\varepsilon_{Nd}(t) = +5.5$ to -4.1), and mafic enclaves and shoshonites have low I_{Sr} (0.7035–0.7040) and high $\varepsilon_{Nd}(t)$ (+5 to +6) values, implying a mixed mantle-continental source. These igneous rocks are interpreted as evidence of the change from Tethysian compression to paleo-Pacific extension, i.e., from crustal-source magma to a mixed crustal-mantle source magma during the Early–Middle Jurassic. Termination of the Tethysian regime probably took place during the early Late Jurassic.

5.2. Middle–Late Jurassic (J_2–J_3): peraluminous granitoids

The inland part of the SECB, especially the Nanling–Wuyishan belt, experienced the beginning of a large-scale granitic magmatism between 180 and 145 Ma (Zhou et al., 2006a), that subsequently controlled the formation of granite ranges and coeval fault-depression basins.

The initial stage of magmatism (180–160 Ma) was caused by underplating of basaltic magma that provided heat for anatexis of Meso-proterozoic quartzofeldspathic sedimentary rocks. The igneous rock product is massive granite that contains few mafic enclaves and is not associated with coeval volcanics (Wang and Zhou, 2002).

Between 160 and 145 Ma, granite magmatism within the whole SECB was constrained by the paleo-Pacific Plate subduction regime. Large-scale NE-trending granitic batholiths are mainly exposed east of Nanling. Some small-scale coeval S-type granitic volcanic-intrusive complexes are developed in South Jiangxi.

The NW-NWW subduction of the paleo-Pacific Plate beneath the eastern Asian continental block resulted in the development of a broad Late Mesozoic active continental margin and extensional zone (Wang and Mo, 1995; Wang and Zhou, 2002). Subduction strongly influenced and reworked the SECB, destroying the pre-Jurassic tectonic framework and shape of the T_3–J_1 basins, building rift basins, faulted-depression basins and generating Late Jurassic peraluminous granitoids.

5.3. Early Cretaceous (K_1): granitic volcanic–intrusive complexes and bimodal volcanism

During the initial stage of the Early Cretaceous, all of the SECB was subjected to the influence of paleo-Pacific Plate subduction tectonics. Low-angle subduction had reached the Gajiang fault zone, so that, the whole SECB became a back-arc extensional environment (Wang and Zhou, 2002; Shu and Zhou, 2002; Zhou and Li, 2000; Zhou et al., 2006b) (Fig. 8).

In this stage, wet partial melting of mantle peridotite of the upper slab is thought to have occurred. Following crustal thinning, underplating of basaltic magmas associated with upwelling of mixed crust-mantle magma under an extensional setting took place to form: (1) large -type granitic volcanic-intrusive

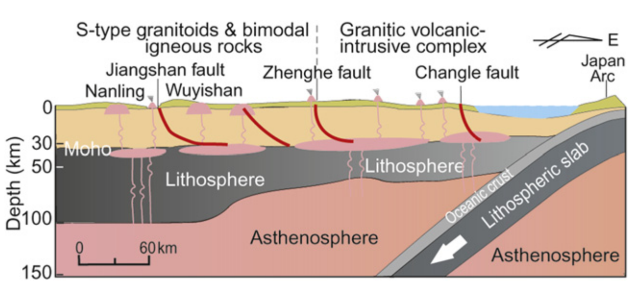

Figure 8 Geodynamic model for formation of Late Mesozoic igneous rocks of the Southeast China block (SECB).

complexes (K_1), (2) bimodal volcanic rocks (K_1), (3) metamorphic core complexes (K_1) and A-type granites or composite magmatic rocks (K_1 and K_2).

It is worth noting that a short-term uplift event occurred in the coastal areas at around 100 Ma. This is indicated by an angular unconformity between Late Cretaceous conglomeratic red beds and coeval volcanic rocks (Charvet et al., 1985, 1999; Lapierre et al., 1997), and was presumably caused by collision between the eastern Asian continental margin and the Philippine Plate as characterized by subduction-type mélanges, ophiolitic nappes and HP/LT type glaucophane-schists in the SW-Japan, Taiwan, Mindoro and the Palawan areas of the Philippines (Minato and Hunahashi, 1985; Ichikawa et al., 1990; Jahn et al., 1990; Lo and Yui, 1996; Maruyama et al., 1997). In response to this collision, some of the pre-Cretaceous granites were uplifted (Shu et al., 2004b, 2009).

5.4. Late Cretaceous–Paleogene (K_2–E): final stage of South China basin and range development

Following short-term Late Cretaceous uplift, the subduction zone of Pacific Plate eastward migrated to the high-angle Japan and Maliana trenchs (Uyeda, 1983; Engebretson et al., 1985; Zhou and Li, 2000; Shu and Zhou, 2002). The width of tectonic disturbance of this high-angle subduction is narrower, and thus subduction-type magmatism produced by melting of the subducting slab did not reach the SECB, and granitic magmatism had ceased since the Late Cretaceous at around 90 Ma (Wang and Zhou, 2002). Since this time, the SECB was further extended and thinned to produce an extensive intra-continental extensional zone of red clastic basins (K_2–E) occupying an area of 40,000 km^2.

The SECB is underlain by a notably thinned lithosphere of about 80 km in coastal areas, 110 km in the Wuyishan area, and 200 km in the Nanling area (Zhou et al., 2006b). This has produced many red bed-filled faulted-depressions with intercalations of alkaline basalt and mafic dykes, dated at 100–90 Ma (Shu et al., 2004a; Yu et al., 2005).

6. Comparison of the basin and range tectonics of South China and the western North America

6.1. Division of tectonic units of western North America

The N–S-trending Cordilleran belt in western North America with a width more than 800 km is a composite tectonic domain produced by Cretaceous–Paleogene subduction and Cenozoic extension. It consists of six tectonic units from west to east as follows (Shu and Wang, 2006): (1) San Andreas transform fault; (2) San Francisco ophiolitic mélange and accretion zone of terranes; (3) Nevada Cretaceous intermediate-acid magmatic arc; (4) basin and range tectonic zone (bimodal volcanic rocks, alkaline basalts and metamorphic core complexes) and Cenozoic Yellowstone mantle plume (mainly alkaline basalts and basalt + rhyolite); (5) foreland thrust zone; and (6) Colorado craton (Proterozoic–Archean crystal basement). Subduction and terrane accretion took place mainly during the Mesozoic–Paleocene. Since 20 Ma the previous collisional orogenic belt was reworked by a regional-scale extension (Hill et al., 1992). Under the influence of the Cenozoic Yellowstone mantle plume, the crust was extended and thinned, from 50% to 300%, forming metamorphic core complexes, bimodal volcanic rocks and alkaline basalts. A regional-scale low-angle normal fault was well developed in the zone of metamorphic core complexes.

Comparison of basin and range tectonics between the SECB and western North America shows some similarities, and also distinct differences, indicating contrastive geological features on both sides of the Pacific Ocean.

6.2. Similarities

Geodynamic mechanism forming the basin and range tectonics on both shores of the Pacific was the same, i.e., both areas were influenced since the Jurassic by Pacific Plate subduction and the strongest influence took place during the Cretaceous. And the active continental margin environments of both areas have a similar width more than 800 km.

The style of basin and range tectonics on both sides of the Pacific is the same, i.e., cordilleran-type that affected the whole crust, and their formation being controlled by a transition from low-angle to a high-angle subduction. Both are the product of back-arc extension tectonics.

6.3. Differences

6.3.1. Mantle plume

The Yellowstone mantle plume of western North America has a diameter more than 1000 km. Extensive alkaline basalt magmatism accompanied by rhyolitic ignimbrite occurred in the basin and range areas to form circular high mountains and some calderas that are less than 5 Ma old. Granite is rare.

Upwelling of the Yellowstone mantle plume caused breakup of the Cordilleran belt and thinning of the lithosphere, leading to eruption of basalt and the development of basin and range tectonics including metamorphic core complexes. Thus, the energy and driving force for basin and range tectonics were derived from this large-scale mantle plume.

There is no evidence for a mantle plume and its associated tectono-magmatic effects in the SECB, although there is evidence for basalt underplating and formation of S-type granitoids. Also, there was minor addition of juvenile mantle material to the continental crust, and metamorphic core complexes are less developed than in western North America.

6.3.2. Extensional scale and magmatic products

Compared with large-scale extension in western North America, the scale of extension in the SECB is notably smaller and the whole of the lithosphere was not affected. Consequently, western North America is marked by the intrusion/eruption of alkaline basalt, while the SECB is characterized by large-scale granite magmatism and less than 10% basaltic rocks.

6.3.3. Geodynamic mechanism of tectonic transformation

Along the eastern Pacific margin, the tectonic transition from low-angle to high-angle subduction ceased during the late Early Cretaceous. High-angle subduction split the eastern Nevada igneous arc, producing many extensional basins. Subduction of the Pacific Plate ended and large extension began in the Miocene (20 Ma) with the upwelling of the Yellowstone mantle plume and the dextral movement on the San Andreas Fault.

Along the western Pacific margin, the tectonic transition from low-angle to high-angle Pacific Plate subduction was associated with a change in the location of the subduction zone. As mentioned above, collision and accretion of the Philippine Plate with the Japan arc along the SW-Japan subduction zone took place in the late Early Cretaceous (Charvet et al., 1985; Jahn, 1974; Jahn et al., 1990). This collision led to a change from low-angle subduction along the SW-Japan trench to high-angle subduction along the Maliana Trench since the Late Cretaceous.

6.3.4. Age of basin and range tectonics

In western North America, large-scale basin and range tectonics began at 18 Ma and ended at 5 Ma. In the SECB, basin and range tectonics began in the Early Cretaceous, and terminated in the Paleogene.

In addition, the red clastic bed-filled basins are very development in the SECB and the deposition of red sediments spans a long-time from the Late Cretaceous to Paleogene (100−20 Ma). In contrast with the SECB, the red rocks in the Late Cretaceous to Paleogene basins are rare in western North America.

7. Conclusions

(1) The results of our study suggest that the SECB experienced a tectonic transition from a Tethysian to paleo-Pacific Plate regime since the late Early Jurassic. Subduction of the paleo-Pacific Plate dominated the tectonics of the SECB since the Early Cretaceous.

(2) Many Late Mesozoic extensional basins and igneous rock assemblages were developed in the SECB under a back-arc extensional setting.

(3) Igneous rocks associated with the SECB extensional setting include intraplate bimodal volcanic rocks of Early−Middle Jurassic ($J_{1\text{-}2}$) age, Middle−Late Jurassic (J_2−J_3) peraluminous granitoids in the inland part of the SECB, Cretaceous (K) granitic volcanic−intrusive complexes and bimodal rocks, together with Late Cretaceous−Paleogene (K_2−E) deposition of red clastic beds and eruption of intercalated alkaline basalt in fault-depression basins. These igneous rock assemblages are considered to reflect significant responses to polyphase tectonic and magmatic events constrained by westward subduction of paleo-Pacific Plate.

(4) Comparison of the basin and range tectonics of the SECB and western North America indicates a similar geodynamic mechanism for the formation and type of basin and range tectonics. But distinct differences also exist between these two areas, such as, mantle plume formation, scales of extensional and igneous rock assemblages, the mechanism of tectonic transformation and the age of basin and range tectonics. These differences are caused mainly by the Yellowstone mantle plume.

Acknowledgements

The authors are grateful to Prof. Mo X.X. (Editor-in-Chief, Geoscience Frontiers) for his invitation to prepare this review paper. Two anonymous reviewers are thanked for their constructive comments, suggestions and English revision, that greatly improved the manuscript. Prof. Zhou X.M. is thanked for providing references and useful suggestions. This research was funded by the National Basic Research Program of China (973 Program, No. 2012CB416701), National Natural Science Foundation of China (Grant 40972132) and was partly supported by the State Key Laboratory for Mineral Deposits Research of Nanjing University (No. 2008-I-01).

References

Bao, Z.W., Zhao, Z.H., Xiong, X.L., 2000. Geochemical features of the Ejinao alkaline syenite and its geodynamic significance. Geochemistry 29 (5), 462−467 (in Chinese with English abstract).

Charvet, J., Faure, M., Caridroit, M., Guidi, A., 1985. Some tectonic and tectonogenetic aspects of SW Japan: an Alpine-type orogen in an island-arc position. In: Nasu, N. (Ed.), Formation of Active Ocean Margin. Terra Science Publication Company, Tokyo, pp. 791−817.

Charvet, J., Lapierre, H., Yu, Y.W., 1994. Geodynamic significance of the Mesozoic volcanism of southeastern China. Journal of Southeast Asian Earth Sciences 9 (4), 387−396.

Charvet, J., Cluzel, D., Faure, M., Shu, L.S., Lu, H.F., 1999. Some tectonic aspects of the pre-Jurassic accretionary evolution of East Asia. In: Metcalfe, I., Ren, J., Charvet, J., Hada, S. (Eds.), Gondwana Dispersion and Asian Accretion. A.A. Balkema, Rotterdam/Brookfield, pp. 37−65.

Charvet, J., Shu, L.S., Faure, M., Choulet, F., Wang, B., Lu, H.F., Le Breton, N., 2010. Structural development of the Lower Paleozoic belt of South China: genesis of an intracontinental orogen. Journal of Asian Earth Sciences 39, 309−330.

Chen, P.R., Kong, X.G., Ni, Q.S., 1999. Ascertainment and implication of the Early Yanshanian Bimodal volcanic association from South Jiangxi Province. Geological Review 45 (Suppl.), 734−741.

Chen, P.R., Hua, R.M., Zhang, B.D., 2002. Post-orogenic Early Yanshanian granotoids in the Nanling Region: petrological constraints and geodynamic settings. Science in China (D) 32 (4), 279−289.

Chen, X., Zhang, Y.D., Fan, J.X., Cheng, J.F., Li, Q.J., 2010. Ordovician graptolite-bearing strata in southern Jiangxi with a special reference to the Kwangsian Orogeny. Science of China (Earth Sciences) 53, 1602−1610.

Chen, Y.H., Chen, Z.B., Chen, Z.Y., 1998. Meso-Cenozoic Extensional Tectonics and Uranium Metallogenesis in Southeast China. Atomic Energy Publishing House, Beijing, pp. 1−262 (in Chinese with English abstract).

Cloetingh, S., Podlachikov, Y., 2000. Basin origin and crustal structure. Tectonophysics 320, 1−432.

Cloetingh, S., Marzo, M., Munoz, J., Verges, A., 2002. Tectonics of sedimentary basins: from Crustal Structure to Basin Fill. Tectonophysics 340, 1−135.

Coney, P.J., 1980. Cordilleran metamorphic core complex: an overview. Memoir of Geological Society of America 153, 7−31.

Crittenden, M.D., 1980. Metamorphic core complexes of the North American Cordillera: summary. Memoir of Geological Society of America 153, 485−490.

Darby, B.J., Davis, G.A., Zheng, Y., 2001. Evolving geometry of the Hohhot metamorphic core complex, Inner Mongolia, China. Journal of Geological Society of America. Abstracts with Programs 33 (3), A32.

Davis, G.H., Coney, P.J., 1979. Geologic development of the Cordilleran metamorphic core complex. Geology 7, 120−124.

Davis, G.A., Arderson, J.L., Frost, E.G., 1980. Mylonitization and detachment faulting in the Whipple-Buckskin-Rawhide Mountains terrane, Southeastern California and Western Arizona. Geological Society of America Memoirs 153, 79−129.

Deng, P., Shu, L.S., Yang, M.G., 2003. Geological features and dynamic evolution of the Ganjiang fault in Jiangxi Province. Geological Review 49 (2), 113−122.

Deng, P., 2003. Study on the geodynamics of the Mesozoic−Cenozoic basin−range evolution in the eastern Nanling belt and their uranium metallization. Ph.D. dissertation, Nanjing University, Nanjing, China, 1−176 (in Chinese with English abstract).

Deng, P., Shu, L.S., Yu, X.Q., 2004. Early−Middle Jurassic Basins and features of volcanic rocks in the Western Fujian-Southern Jiangxi region. Acta Petroligica Sinica 20 (3), 521−532.

Dickinson, W.R., 2002. The basin and range province as a composite extensional domain. International Geology Review 44, 1−38.

Engebretson, D.C., Cox, A., Gordon, R.G., 1985. Relative Motions Between Oceanic and Continental Plates in the Pacific Basin. Geological Society of America, Spec Paper, pp. 1−59.

Faure, M., Sun, Y., Shu, L.S., Charvet, J., 1996. Extensional tectonics within a subduction-type orogen: the case study of the Wugongshan dome (Jiangxi Province, Southeastern China). Tectonophysics 263, 77−106.

Faure, M., Shu, L.S., Wang, B., Charvet, J., Choulet, F., Monié, P., 2009. Intracontinental subduction: a possible mechanism for the Early Palaeozoic Orogen of SE China. Terre Nova 21, 360−368.

Gilder, S.A., Keller, G.R., Luo, M., 1991. Eastern Asia and the western Pacific timing and spatial distribution of rifting in China. Tectonophysics 197, 225−243.

Guo, L.Z., Yu, J.H., Shi, Y.S., 1965. Main features of tectonic development of the Caledonian period folded geosyncline, South China (in Chinese with English abstract). In: Geotectonic Problems of China. Science Press, Beijing, pp. 165−183.

Guo, L.Z., Shi, Y.S., Ma, R.S., 1980. Geotectonic framework and crust evolution of the South China. In: Scientific Papers on Geology for International Exchange (I) (in Chinese with English abstract). Geological Publishing House, Beijing, pp. 109−116.

Guo, L.Z., Shi, Y.S., Lu, H.F., Ma, R.S., Dong, H.G., Yang, S.F., 1989. The pre-Devonian tectonic patterns and evolution of South China. Journal of Southeast Asian Earth Sciences 3, 87−93.

Hill, E.J., Baldwin, S.L., Lister, G.S., 1992. Unroofing of active metamorphic core complexes in the D'Entrecasteau Islands, Papua New Guinea. Geology 20, 907−910.

Huang, T.K., 1945. On major tectonic forms of China. Geological Memoirs, Nanjing, Series A (20), 1−165.

Ichikawa, K., Mizutani, S., Hara, I., 1990. Pre-Cretaceous terranes of Japan. Publ. IGCP 224: Pre-Jurassic Evolution of Eastern Asia, Osaka, pp. 1−413.

Jahn, B.M., Zhou, X.H., Li, J.L., 1990. Formation and tectonic evolution of southeastern China and Taiwan: isotopic and geochemical constraints. Tectonophysics 183, 145−160.

Jahn, B.M., 1974. Mesozoic thermal events in Southeast China. Nature 248, 480−483.

Lapierre, H., Jahn, B.M., Charvet, J., Yu, Y.W., 1997. Mesozoic felsic arc magmatism and continental olivine tholeiites in Zhejiang Province and their relationship with tectonic activity in SE China. Tectonophysics 274, 321−338.

Li, T.D., 2010. The principal characteristics of the lithosphere of China. Geoscience Frontier 1 (1), 45−56.

Li, W.X., Li, X.H., Li, Z.X., 2005. Neoproterozoic bimodal magmatism in the Cathaysia Block of South China and its tectonic significance. Precambrian Research 136, 51−66.

Li, X.H., 2000. Cretaceous magmatism and lithospheric extension in Southeast China. Journal of Asian Earth Sciences 18, 293−305.

Li, X.H., Sun, M., Wei, G.J., LiuLee, C.Y., Malpas, J., 2000. Geochemical and Sm−Nd isotopic study of amphibolites in the Cathaysia block, southeastern China: evidence for an extremely depleted mantle in the Paleoproterozoic. Precambrian Research 102, 251−262.

Li, Z.X., Li, X.H., Wartho, J.A., Clark, C., Li, W.X., Zhang, C.L., Bao, C.M., 2010. Magmatic and metamorphic events during the Early Paleozoic Wuyi-Yunkai Orogeny, southeastern South China: new age constraints and P-T conditions. Geological Society of America Bulletin 122 (516), 772−793.

Lister, G.S., Baldwin, S.L., 1993. Plutonism and the origin of metamorphic core complexes. Geology 21, 607−610.

Lo, C., Yui, T.H., 1996. $^{40}Ar/^{39}Ar$ dating of high-pressure rocks in the Tananao basement complex, Taiwan. Journal of Geological Society of China 39 (1), 13−30.

Lou, F.S., Shen, W.Z., Wang, D.Z., Shu, L.S., Wu, F.J., Zhang, F.R., Yu, J.H., 2005. Zircon U-Pb isotopic chronology of the Wugongshan dome compound granite in Jiangxi Province. Acta Geologica Sinica 79 (5), 636−644.

Liu, J.H., Wu, H., Liu, F.T., 1996. Features of 3-D velocity distribution and lithosphere structure in South China and its contiguous sea area. Acta Geophysica Sinica 39 (4), 483−492.

Maruyama, S., Isozaki, Y., Kimura, G., Terabayashi, M., 1997. Paleogeographic maps of the Japanese islands: plate tectonic synthesis from 750 Ma to the present. The Island Arc 6 (1), 121−142.

Miller, J.A., Holdsworth, R.E., Buick, I.S., Hand, M., 2001. Continental Reactivation and Reworking. Journal of the Geological Society Special Publication, London, vol. 184, 1−394.

Minato, M., Hunahashi, M., 1985. Crustal structure of the Japanese islands, Japan Sea, coastal part of western Pacific and Phillippine Sea. Bulletin of Japan Sea Research Institute, Kanazawa University (17), 13−42.

Qiu, J.S., Wang, D.Z., McInnes, B.I.A., Jiang, S., Wang, R.C., Kanisawa, S., 2004. Two subgroups of A-type granites in the coastal area of Zhejiang and Fujian Provinces, SE China: age and geochemical constraints on their Petrogenesis. Transactions of the Royal Society of Edinburgh: Earth Sciences 95, 227−236.

Qiu, J.S., Wang, D.Z., McInnes, B.I.A., 2000a. A-type granites in the coastal area of Fujian Provinces, SE China: geochemical constraints on their petrogenesis. Geochemistry 29 (4), 313−321 (in Chinese with English abstract).

Qiu, J.S., Wang, D.Z., Zhou, J.C., Wang, R.C., 2000b. Ascertainment of the alkaline rhyolites at Yunshan, Yongtai County, Fujian Province and its geological significance. Geological Review 46 (5), 520−529 (in Chinese with English abstract).

Ren, J.S., 1964. Preliminary discussion on several problems of Caleodonian tectonics of the Southeastern China. Acta Geologica Sinica 44 (4), 418−430.

Ren, J.S., Chen, T., 1989. Tectonic evolution of the continental lithosphere in eastern China and adjacent areas. Journal of Southeast Asian Earth Sciences 3, 17−27.

Rong, J.Y., Zhan, R.B., Xu, H.G., Huang, B., Yu, G.H., 2010. Expansion of the Cathaysian Oldland through the Ordovician−Silurian transition: emerging evidence and possible dynamics. Science of China (D) 53, 1−17.

Shu, L.S., Sun, Y., Wang, D.Z., Faure, M., Monie, P., Charvet, J., 1998. Mesozoic doming extentional tectonics of Wugongshan, South China. Science in China (Series D) 41 (6), 601−608.

Shu, L.S., Yu, J.H., Wang, D.Z., 2000. Late Mesozoic granitic magmatism and metamorphism-ductile deformation in the Changle−Nanao fault zone, Fujian Province. Geological Journal of China Universities 6 (3), 368−378.

Shu, L.S., Zhou, X.M., 2002. Late Mesozoic tectonism of Southeast China. Geological Review 48 (3), 249−260 (in Chinese with English abstract).

Shu, L.S., Deng, P., Wang, B., Tan, Z.Z.G., Yu, X.Q., Sun, Y., 2004a. Lithology, kinematics and geochronology related to Late Mesozoic Basin-Mountain evolution in the Nanxiong-Zhuguang Area, South China. Science in China (D) 47 (8), 673−688.

Shu, L.S., Zhou, X.M., Deng, P., Yu, X.Q., Wang, B., Zhu, F.P., 2004b. Geological features of Mesozoic−Cenozoic basins and their tectonic evolution in Southeast China. Geological Bulletin of China 23 (9−10), 876−884 (in Chinese with English abstract).

Shu, L.S., 2006. Pre-Devonian tectonic evolution of South China: from Cathaysia block to Caledonian Period folded orogenic belt. Geological Journal of China Universities 12, 418−431 (in Chinese with English abstract).

Shu, L.S., Wang, D.Z., 2006. A comparison study of basin and range tectonics in the Western North America and Southeastern China. Geological Journal of China Universities 12 (1), 1−13 (in Chinese with English abstract).

Shu, L.S., Faure, M., Wang, B., Zhou, X.M., Song, B., 2008a. Late Paleozoic−Early Mesozoic geological features of South China: response to the Indosinian collision event in Southeast Asia. Comptes Rendus des Geosciences 340, 151−165.

Shu, L.S., Deng, P., Yu, J.H., Wang, Y.B., Jiang, S.Y., 2008b. The age and tectonic environment of the rhyolitic rocks on the western side of Wuyi Mountain, South China. Science of China (D) 51 (8), 1053−1063.

Shu, L.S., Yu, J.H., Jia, D., Wang, B., Shen, W.Z., Zhang, Y.Q., 2008c. Early Paleozoic orogenic belt in the eastern segment of South China. Geological Bulletin of China 27 (10), 1081−1093.

Shu, L.S., Zhou, X.M., Deng, P., Wang, B., Jiang, S.Y., Yu, J.H., Zhao, X.X., 2009a. Mesozoic tectonic evolution of the southeast china block: new insights from basin analysis. Journal of Asian Earth Sciences 34, 376–391.

Shu, L.S., Wang, Y., Sha, J.G., Jiang, S.Y., Yu, J.H., 2009b. Jurassic sedimentary features and tectonic settings of southeast China. Science in China (D) 52 (12), 1969–1978.

Shu, L.S., Faure, M., Yu, J.H., Jahn, B.M., 2011. Geochronological and geochemical features of the Cathaysia block (South China): new evidence for the Neoproterozoic breakup of Rodinia. Precambrian Research 187, 263–276.

Sun, T., 2006. A new map showing the distribution of granites in South China and its explanatory noes. Geological Bulletin of China 25 (3), 332–335.

Uyeda, S., 1983. Comparative subductology. Episodes 2, 19–24.

Wang, D.Z., Zhao, G.T., Qiu, J.S., 1995. The tectonic constraint on the Late Mesozoic A-type granitoids in Eastern China. Geological Journal of China Universities 1 (2), 13–21 (in Chinese with English abstract).

Wang, D.Z., Shu, L.S., Faure, M., Sheng, W.Z., 2001. Mesozoic magmatism and granitic dome in the Wugongshan Massif, Jiangxi Province and their genetical relationship to the tectonic events in Southeast China. Tectonophysics 339, 259–277.

Wang, D.Z., Zhou, X.M., 2002. Genesis of Late Mesozoic Volcanic–Intrusive Complex of Southeast China and Crustal Evolution. Science Press, Beijing, pp. 1–295.

Wang, D.Z., Shen, W.Z., 2003. Genesis of granitoids and crustal evolution in southeast China. Earth Science Frontiers 10 (3), 209–220 (in Chinese with English abstract).

Wang, H.Z., Mo, X.X., 1995. An outline of the tectonic evolution of China. Episodes 18 (1–2), 6–16.

Wang, Z.H., Lu, H.F., 2000. Ductile deformation and $^{40}Ar/^{39}Ar$ dating of the Changle–Nanao ductile shear zone, southeastern China. Journal of Structural Geology 22, 561–570.

Wernicke, B., 1981. Low-angle normal faults in the Basin and Range province: nappe tectonics in an extending orogen. Nature 291, 645–648.

Wernicke, B., 1985. Uniform-sense normal simple shear of the continental lithosphere. Canadian Journal of Earth Sciences 22, 108–125.

Xiang, L., Shu, L.S., 2010. Predevonian tectonic evolution of the eastern South China block: geochronological evidence from detrital zircons. Science in China (Earth Sciences) 53 (10), 1427–1444.

Xu, K.Q., Liu, Y.J., Yu, S.J., 1960. Discussion on the Caledonian Period Granite in South Jiangxi. Geological Review 20, 112–114 (in Chinese with English abstract).

Xu, M.J., Shu, L.S., 2001. A deep geological setting constraining the Late-Mesozoic magmatism in the SE-China. Geological Journal of China Universities 7 (1), 21–33 (in Chinese with English abstract).

Xu, X.S., Deng, P., O'Reilly, S.Y., 2003. The laser probe ICPMS U-Pb dating on single zircon grains from the Guidong granitic complexes, South China and their petrological implication. Chinese Science Bulletin 48 (12), 1328–1334 (in Chinese).

Yao, J.L., Shu, L.S., Santosh, M., 2011. Detrital zircon U-Pb geochronology, Hf-isotopes and geochemistry—new clues for the Precambrian crustal evolution of Cathaysia Block, South China. Gondwana Research 20, 553–567.

Yu, J.H., Wang, L.J., Griffin, W.L., O'Reilly, S.Y., Zhang, M., Li, C.Z., Shu, L.S., 2009. A Paleoproterozoic orogeny recorded in a long-lived cratonic remnant (Wuyishan terrane), eastern Cathaysia Block, China. Precambrian Research 174, 347–363.

Yu, X.Q., Shu, L.S., 2004. Late Mesozoic crustal evolution of the Ganhang belt, South China: constraints from geochemistry of volcanic rocks. Geochimica et Cosmochimica Acta 68 (11s), A723.

Yu, X.Q., Shu, L.S., Yan, T.Z., Zu, F.P., 2005. Prototype and sedimentation of red basins along the Ganhang tectonic belt. Acta Sedimentologica Sinica 23 (1), 12–20.

Yu, Y.W., Xu, B.T., 1999. The sequence and age of Late Mesozoic volcanic-sedimentary rock series in Zhejiang Province. Journal of Stratigraphy 23 (2), 136–145 (in Chinese with English abstract).

Zhang, Y., Shu, L.S., 2011. Study of geochemistry, geochronology and petro-genesis of the Early Paleozoic granitic plutons in the central-southern Jiangxi Province. Science in China (Earth Sciences) 54 (10), 1492–1510.

Zhao, D.P., Liu, L., 2010. Deep structure and origin of active volcanoes in China. Geoscience Frontiers 1 (1), 31–44.

Zhou, J.C., Chen, R., 2000. Late Mesozoic interaction between crust and mantle in coastal area of Zhejiang–Fujian. Progress in Natural Sciences 10 (9), 713–717.

Zhou, J.C., Chen, R., 2001. Geochemistry of late Mesozoic interaction between crust and mantle in southeastern Fujian province. Geochimica 30 (6), 547–558 (in Chinese with English abstract).

Zhou, J.C., Jiang, S.Y., Wang, X.L., 2005. Re-Os isochron age of Fankeng basalts from Fujian of SE China and its geological significance. Geochemical Journal 39 (6), 497–502.

Zhou, J.C., Jiang, S.Y., Wang, X.L., Yang, J.H., Zhang, M.Q., 2006a. Study on lithogeochemistry of Middle Jurassic basalts from southern China represented by the Fankeng basalts from Yongding of Fujian Province. Science in China (Earth Sciences) 49 (10), 1020–1031.

Zhou, X.M., Li, W.X., 2000. Origin of Late Mesozoic igneous rocks in Southeastern China: implications for lithosphere subduction and underplating of mafic magmas. Tectonophysics 326, 269–287.

Zhou, X.M., Sun, T., Shen, W.Z., Shu, L.S., Niu, Y.L., 2006b. Petrogenesis of Mesozoic granitoids and volcanic rocks in South China: a response to tectonic evolution. Episodes 29 (1), 26–33.

Zhou, X.M., 2007. Genesis of Late Mesozoic Granitoids in the Nanling Region and the Lithospheric Dynamic Evolution. Science Press, Beijing, pp. 1–691 (in Chinese with English abstract).